MCB
Journals.ASM.org

Mitochondrial Fission Contributes to Mitochondrial Dysfunction and Insulin Resistance in Skeletal Muscle

Huei-Fen Jheng,[a] Pei-Jane Tsai,[b] Syue-Maio Guo,[c] Li-Hua Kuo,[a] Cherng-Shyang Chang,[a] Ih-Jen Su,[d,e] Chuang-Rung Chang,[f] and Yau-Sheng Tsai[a,c,g]

Institute of Basic Medical Sciences,[a] Department of Medical Laboratory Science and Biotechnology,[b] Institute of Clinical Medicine,[c] Department of Pathology,[d] and Cardiovascular Research Center,[g] College of Medicine, National Cheng Kung University, Tainan, Division of Infectious Diseases, National Health Research Institues, Tainan,[e] and Institute of Biotechnology, National Tsing Hua University, Hsinchu,[f] Taiwan, Republic of China

Mitochondrial dysfunction in skeletal muscle has been implicated in the development of insulin resistance and type 2 diabetes. Considering the importance of mitochondrial dynamics in mitochondrial and cellular functions, we hypothesized that obesity and excess energy intake shift the balance of mitochondrial dynamics, further contributing to mitochondrial dysfunction and metabolic deterioration in skeletal muscle. First, we revealed that excess palmitate (PA), but not hyperglycemia, hyperinsulinemia, or elevated tumor necrosis factor alpha, induced mitochondrial fragmentation and increased mitochondrion-associated Drp1 and Fis1 in differentiated C2C12 muscle cells. This fragmentation was associated with increased oxidative stress, mitochondrial depolarization, loss of ATP production, and reduced insulin-stimulated glucose uptake. Both genetic and pharmacological inhibition of Drp1 attenuated PA-induced mitochondrial fragmentation, mitochondrial depolarization, and insulin resistance in C2C12 cells. Furthermore, we found smaller and shorter mitochondria and increased mitochondrial fission machinery in the skeletal muscle of mice with genetic obesity and those with diet-induced obesity. Inhibition of mitochondrial fission improved the muscle insulin signaling and systemic insulin sensitivity of obese mice. Our findings indicated that aberrant mitochondrial fission is causally associated with mitochondrial dysfunction and insulin resistance in skeletal muscle. Thus, disruption of mitochondrial dynamics may underlie the pathogenesis of muscle insulin resistance in obesity and type 2 diabetes.

The prevalence of obesity and type 2 diabetes is increasing at an alarming rate in industrialized countries, partly due to excess food intake and physical inactivity. Excess dietary fat and sugar leads to increased flux of energy fuel substrates and increased lipid burden in peripheral tissues. Skeletal muscle is the major site of glucose uptake and metabolism. Increased fatty acid (FA) uptake contributes to increased lipid accumulation in skeletal muscle, leading to lipotoxicity, which is known to impair muscle insulin sensitivity (2, 20). In addition, the intracellular lipid metabolites have been shown to activate serine/threonine protein kinases and suppress insulin actions (37).

Mitochondria are important organelles for cellular function through regulation of energy metabolism, ATP generation, and calcium handling. Substantial evidence shows that mitochondrial dysfunction and impairment of the oxidative capacity in skeletal muscle are key mechanisms mediating insulin resistance (24, 34). A reduction in the number and function of mitochondria has been documented in the skeletal muscle of type 2 diabetic patients and animals. For example, the activity of the electron transport chain in subsarcolemmal mitochondria is dramatically reduced in type 2 diabetic and obese subjects, compared with that in lean subjects (36). Furthermore, patients with severe insulin resistance exhibit decreased mitochondrial oxidative activity and ATP synthesis in skeletal muscle (22, 34). High-fat diets downregulate the genes related to mitochondrial biogenesis and the electron transport chain in muscle tissues from mice and humans (3, 40), suggesting that excess dietary fat impairs mitochondrial biogenesis and function.

Mitochondria constantly fuse and divide, processes known as fusion and fission, leading to dynamic networks of mitochondria. The frequencies of fusion and fission events are balanced to maintain the overall morphology of the mitochondrial population (8, 41). A high fusion-to-fission ratio leads to elongated, tubular, interconnected mitochondrial networks, whereas a low ratio results in fragmented, discontinuous mitochondria. These two opposing processes are finely regulated by the mitochondrial fusion proteins mitofusins 1 and 2 (Mfn1 and Mfn2, respectively) and optic atrophy 1 (Opa1) and by the mitochondrial fission proteins dynamin-related protein 1 (Drp1) and fission protein 1 (Fis1).

Recent work has highlighted the importance of mitochondrial fusion and fission in cellular function and animal physiology (13, 41). For example, fibroblasts lacking Mfn1 and Mfn2 completely lack mitochondrial fusion and show severe cellular defects, including poor growth, heterogeneity of mitochondrial membrane potential, and decreased respiration (11). Lack of fission by downregulation of Drp1 expression leads to loss of mitochondrial DNA (mtDNA) and a decrease in mitochondrial respiration in HeLa cells (33). However, another study demonstrated that inhibition of Drp1 prevents the decrease in mitochondrial membrane potential and release of cytochrome *c* in COS-7 cells (16). Nevertheless, balanced mitochondrial dynamics is critical to maintenance of functional mitochondria, energy generation, and prevention of apoptosis.

Although decreased mitochondrial function and activity in

Received 10 May 2011 **Returned for modification** 31 May 2011
Accepted 6 November 2011
Published ahead of print 14 November 2011
Address correspondence to Yau-Sheng Tsai, yaustsai@mail.ncku.edu.tw.
Supplemental material for this article may be found at http://mcb.asm.org/.

doi:10.1128/MCB.05603-11

skeletal muscle has been documented in obesity and type 2 diabetes, the involvement of mitochondrial dynamics in the pathogenesis of metabolic disorders remains unclear. In this study, we hypothesized that obesity and excess energy intake shift the balance of mitochondrial dynamics, further contributing to mitochondrial dysfunction and metabolic deterioration in skeletal muscle. Therefore, we designed experiments to examine the cellular and physiological significance of the continual fusion and fission of mitochondria in response to metabolic overload.

MATERIALS AND METHODS

Mice. Leptin-deficient (*ob*/*ob*) mice and control littermates, obtained from The Jackson Laboratory, were fed regular chow (Purina Laboratory Rodent Diet 5001; PMI Nutrition International, Richmond, IN). For the diet-induced obese group, 8-week-old male C57BL/6 mice, obtained from National Laboratory Animal Center (Tainan, Taiwan), were fed a high-fat (HF) diet (58R2; TestDiet, Richmond, IN) or a control low-fat (LF) diet (58R0; TestDiet). Animals were housed in a specific-pathogen-free barrier facility and handled in accordance with procedures approved by the Institutional Animal Care and Use Committees of the National Cheng Kung University.

Cell culture. Mouse C2C12 myoblasts were maintained in Dulbecco's modified Eagle's medium (DMEM) supplemented with 10% fetal bovine serum. Cells were differentiated by replacing the medium with DMEM containing 2% horse serum. After 3 days of differentiation, C2C12 cells expressing the muscle marker desmin were starved for 4 h and then transferred to serum-free DMEM containing 2% bovine serum albumin with or without FAs (Sigma-Aldrich, St. Louis, MO). No effect of FAs on cell viability under this experimental condition was identified. C2C12 cells on day 2 after differentiation were transfected with a plasmid expressing Drp1-K38A (9) or a control plasmid (pCDNA3) using the Neon transfection system (Invitrogen, Carlsbad, CA). Knockdown of Drp1 was performed on 1 day postdifferentiation C2C12 cells transfected with a *Drp1* short hairpin RNA (shRNA) (TRCN0000321167) or a control shRNA (pLKO.1-shLuc) plasmid using the TurboFect transfection system (Fermentas, Glen Burnie, MD).

Mitochondrial morphology. Transmission electron microscopy was performed on 90-nm sections from mouse gastrocnemius muscle with a Hitachi 7000 transmission electron microscope. Mitochondrial area and length in the gastrocnemius skeletal muscle were measured in 400 mitochondria per mouse using ImageJ software. Mitochondrial morphology was examined in C2C12 cells stained with 200 nM MitoTracker Green FM (Molecular Probes, Eugene, OR) with a fluorescence microscope (Olympus, Tokyo, Japan) or a confocal microscope (C1-Si; Nikon, Tokyo, Japan). For the quantification of tubular mitochondrial morphology, at least 100 randomly chosen cells per treatment group were designated as being either elongated all over (100%), predominantly elongated (80%), modestly elongated (60%), predominantly fragmented (40%), or fragmented all over (20%) over three independent experiments by two investigators blinded to the treatment. For the real-time recording of mitochondrial morphology, cells were visualized with a confocal microscope with a 60× objective lens, and the images were taken every 30 s after treatment with different medium for 1 h.

Mitochondrial extraction. The mitochondrial fraction was isolated as previously described (6). Briefly, tissues and cells were collected and homogenized in a buffer consisting of 250 mM sucrose, 0.5 mM EGTA, 0.5 mM EDTA, and 3 mM HEPES-NaOH (pH 7.2). The homogenate was centrifuged at 800 × *g* for 10 min at 4°C. The supernatant was transferred and centrifuged again at 10,000 × *g* for 10 min at 4°C. The pellet containing mitochondria was resuspended.

Immunoblot analysis. Proteins were subjected to electrophoresis, transferred to polyvinylidene difluoride membranes, and probed with antibodies against Mfn1 and Opa1 (Abnova, Taipei, Taiwan); Mfn2 (Sigma-Aldrich); Drp1 (BD Biosciences, Franklin Lakes, NJ); Fis1 (Biovision, Mountain View, CA); insulin receptor substrate 1 (IRS-1) phospho-Tyr608 (Abcam, Cambridge, MA); IRS-1 (Millipore, Billerica, MA); and Akt phospho-Ser473, Akt, glycogen synthase kinase 3 α subunit (GSK-3α) phospho-Ser21, GSK-3, extracellular signal-regulated kinases 1/2 (ERK1/2) phospho-Thr202/204, ERK1/2, p38 phospho-Thr180/Tyr182, p38, c-Jun N-terminal kinases (JNK) phospho-Thr183/Tyr185, and JNK (Cell Signaling, Danvers, MA). Immunoreactive proteins were detected using an enhanced chemiluminescence Western blotting detection system (Millipore).

Quantitative RT-PCR and mtDNA content analyses. Total RNA was extracted using REzol (PROtech, Mukilteo, WA). Samples of mRNA were analyzed by SYBR green-based real-time quantitative reverse transcription (RT)-PCR (Applied Biosystems, Foster City, CA) with the gene for cyclophilin A as the reference in each reaction. Total DNA was extracted from cells using a genomic DNA isolation kit (Geneaid, Taipei, Taiwan). The mtDNA content was calculated using real-time quantitative PCR by measuring a mitochondrial gene (*Cox1*) versus a nuclear gene (*Gapdh*).

ROS production, mitochondrial polarization, and ATP content. The intracellular level of reactive oxygen species (ROS) was detected using the fluorescent probe H_2DCFDA (25 μM; Sigma-Aldrich). Mitochondrial polarization in cells was analyzed using the cationic fluorescent dye JC-1 (1.5 μM; Molecular Probes). Total ATP content was determined using ATP bioluminescent assay kit (Molecular Probes).

Glucose uptake assay. After treatment with or without palmitate (PA), C2C12 cells were incubated in phosphate-buffered saline (PBS) in the presence or absence of 10 nM insulin for 30 min. Glucose uptake was determined by adding the fluorescent D-glucose analog 2-[*N*-(7-nitrobenz-2-oxa-1,3-diazol-4-yl)amino]-2-deoxyglucose (200 μM; Molecular Probes) for 15 min. After washing with PBS, glucose uptake was measured with a microplate fluorometer (Fluoroskan Ascent; Thermo) and images were captured with a fluorescence microscope (Olympus) with a 10× objective lens.

Glucose tolerance test. Mice were fasted for 4 h and given an oral glucose bolus (2 g/kg body weight). Blood samples were collected before and at indicated times after injections. Plasma glucose concentration was determined with a colorimetric glucose test (Autokit Glucose; Wako, Osaka, Japan). Insulin was measured using mouse insulin enzyme-linked immunosorbent assay (Mercodia, Uppsala, Sweden). The insulin resistance index was calculated as the product of the areas under the glucose and insulin curves in the glucose tolerance test.

Mdivi-1 preparation. Mitochondrial division inhibitor 1 (Mdivi-1; Enzo Life Sciences, Plymouth Meeting, PA) was dissolved in dimethyl sulfoxide. For the *in vitro* experiment, C2C12 cells were incubated with Mdivi-1 for 1 h before analyses of mitochondrial morphology, ROS production, and mitochondrial polarization. For the *in vivo* experiment, mice were fasted for 16 h and intraperitoneally received Mdivi-1 (44 mg/kg in PBS) twice (16 h and 1 h) prior to insulin stimulation or glucose overload.

Data analysis. Values are reported as means ± the standard errors of the means. Statistical analyses were conducted by two-way analysis of variance with treatment and set of experiment as factors. Student's *t* test was used for comparisons between groups within each experiment, and differences were considered to be statistically significant at $P < 0.05$.

RESULTS

External factors involved in the change of mitochondrial morphology. Alterations in the extracellular milieu, including hyperglycemia, hyperinsulinemia, elevated free FAs (FFAs), and elevated proinflammatory cytokines, cause muscle insulin resistance in obesity and type 2 diabetes (18, 31). To investigate whether these external factors directly alter mitochondrial dynamics, we used differentiated C2C12 skeletal muscle cells and screened for putative factors involved in the alteration of mitochondrial dynamics. After staining with MitoTracker Green, C2C12 muscle cells exhibited an interconnected network of tubular, elongated structures. No difference in the tubular feature of mitochondrial

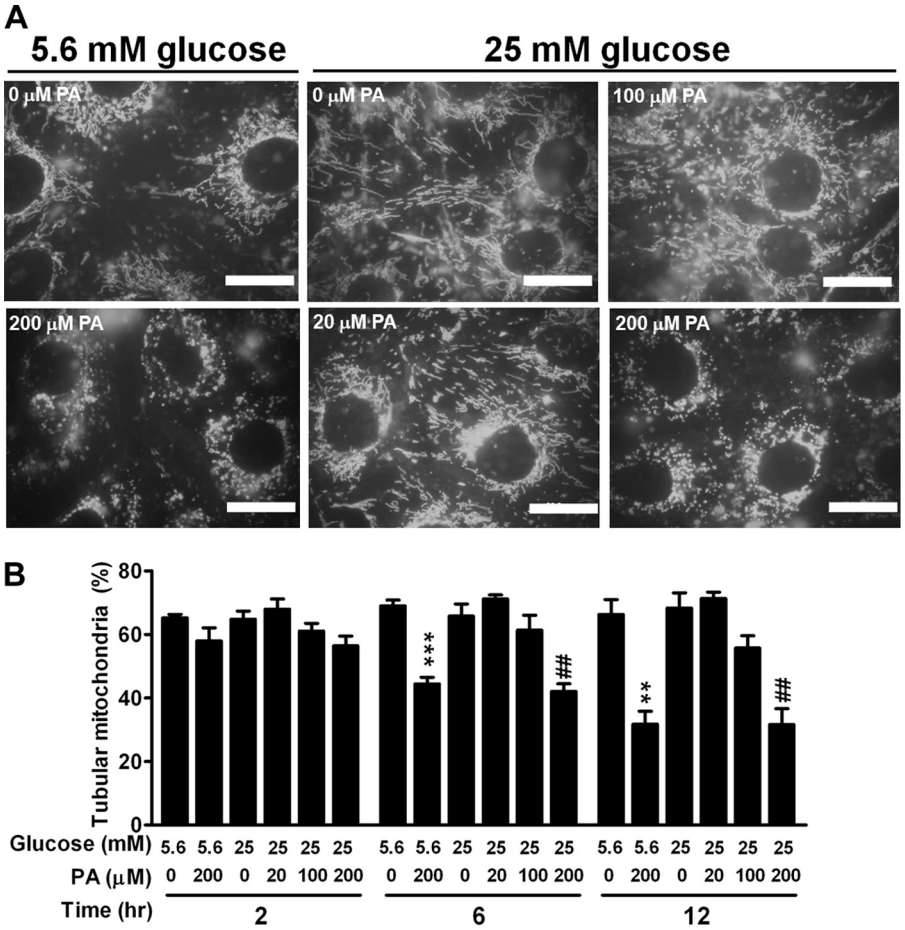

FIG 1 External factors altering mitochondrial morphology in C2C12 cells. (A) Images of C2C12 cells stained with MitoTracker Green after 12 h of incubation in medium containing 5.6 mM or 25 mM glucose with various concentrations of PA ranging from 0 to 200 μM. Each scale bar is 20 μm. (B) Percentage of tubular mitochondria in C2C12 cells incubated in media with various concentrations of glucose and PA for 2, 6, or 12 h. Results are averages of three individual experiments with at least 100 cells per treatment group in each experiment. **, $P < 0.01$; ***, $P < 0.001$ (versus cells treated with 5.6 mM glucose alone). ##, $P < 0.01$ (versus cells treated with 25 mM glucose alone).

morphology was observed between cells treated with a low glucose concentration (5.6 mM) and those treated with a high glucose concentration (25 mM) for 12 h (Fig. 1A). The tubular feature was maintained when cells were treated with a higher glucose concentration of 33 mM for 84 h (data not shown). Similarly, incubation for 12 h at high concentrations of insulin (up to 1.2 μM) and tumor necrosis factor alpha (TNF-α; up to 1 pM) was without effect on the change of mitochondrial tubular feature (data not shown). In contrast, mitochondrial morphology was shifted toward a fragmented, discontinuous network, with a higher proportion of smaller and rounder mitochondria, when cells were treated with one of the most abundant FAs, PA (Fig. 1A). Quantification of the mitochondrial tubular feature, according to the method described by Brooks et al. (5), revealed that treatment with PA shifted mitochondrial morphology toward a fission type in a time- and dose-dependent manner (Fig. 1B). Time-lapse recording demonstrated that mitochondria of the vehicle-treated group exhibited frequent fusion and fission, and the tubular feature of mitochondria was maintained within the time of recording (see video S1 in the supplemental material). In contrast, normal tubular mitochondria underwent fission and became short and small in response to PA treatment. These data suggest that FAs, particularly PA, are an external factor altering mitochondrial dynamics and shifting the balance toward fission in muscle cells.

Differential effects of saturated and unsaturated FAs on mitochondrial morphology. To determine whether different FAs exhibit differential effects on the change in mitochondrial morphology and dynamics, we treated cells with saturated FAs, including myristate (MA; $C_{14:0}$) and stearate (SA; $C_{18:0}$); unsaturated FAs, including palmitoleate (PLA; $C_{16:1}$), oleate (OA; $C_{18:1}$), and linoleate (LA; $C_{18:2}$); and ω-3 polyunsaturated FA docosahexaenoate (DHA; $C_{22:6}$) at 200 μM for 6 h or 12 h. Treatment of C2C12 cells with SA and all of the unsaturated FAs (PLA, OA, and LA) did not alter the mitochondrial tubular morphology (Fig. 2A). However, mitochondrial fragmentation was observed in the groups treated with MA for 6 h and 12 h, which was similar to the effect on the groups treated with PA. Cotreatment with the unsaturated FAs OA and LA and the polyunsaturated FA DHA, but not with the saturated FA SA, attenuated PA-induced mitochondrial fragmentation in C2C12 cells (Fig. 2B). These data indicate that saturated FAs, including MA and PA, lead to mitochondrial fragmentation, whereas unsaturated and polyunsaturated FAs protect against PA-induced mitochondrial fragmentation.

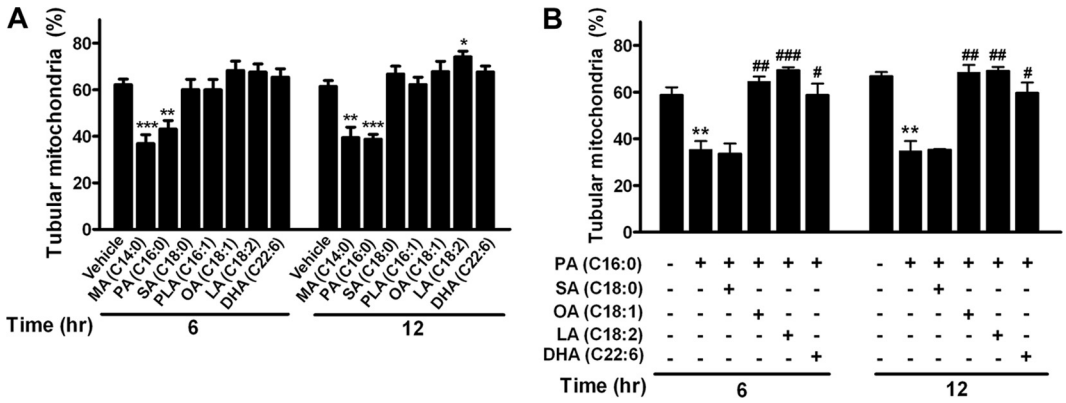

FIG 2 Differential effects of saturated and unsaturated FAs on mitochondrial morphology. (A) Percentage of tubular mitochondria in C2C12 cells treated with various FAs at 200 μM for 6 or 12 h. Saturated FAs include MA, PA, and SA; unsaturated FAs include PLA, OA, and LA; and polyunsaturated FA includes DHA. (B) Percentage of tubular mitochondria in C2C12 cells treated with PA in the presence or absence of other indicated FAs (200 μM) for 6 or 12 h. *, $P < 0.05$; **, $P < 0.01$; ***, $P < 0.001$ (versus vehicle). #, $P < 0.05$; ##, $P < 0.01$; ###, $P < 0.001$ (versus PA alone).

Mitochondrial dysfunction but no change in mitochondrial content due to treatment with PA. To investigate whether the occurrence of mitochondrial fragmentation is associated with mitochondrial dysfunction, we examined mitochondrial membrane potential and total ATP content. Treatment with PA for 6 h and 12 h significantly decreased the mitochondrial membrane potential of C2C12 cells. Cotreatment with DHA completely reversed the decrease in mitochondrial membrane potential (Fig. 3A). Consistently, the total ATP content, reflecting cellular energy production, was decreased in the presence of PA, and this phenomenon was reversed by cotreatment with DHA (Fig. 3B). Thus, these results suggest that mitochondrial fragmentation induced by PA is accompanied by mitochondrial depolarization and loss of ATP production, the characteristics of mitochondrial dysfunction.

Next, we tested whether PA-induced mitochondrial fragmentation and dysfunction were the consequence of reduced mitochondrial content. The ratio of mtDNA to nuclear DNA was not different between the groups treated with and without PA. Cotreatment with DHA also did not alter the ratio of mtDNA to nuclear DNA, compared to that of the other two groups (Fig. 3C). The expression of genes related to mitochondrial biogenesis, including peroxisome proliferator-activated receptor gamma coactivator 1 alpha (*Ppargc1a*), mitochondrial transcription factor A (*Tfam*), and estrogen-related receptor alpha (*Esrra*), and mtDNA

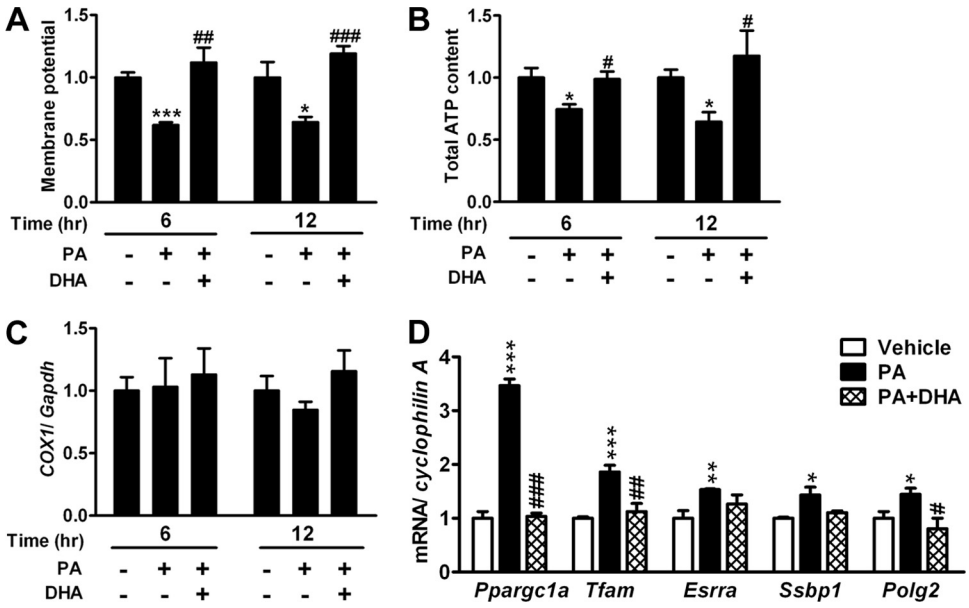

FIG 3 Mitochondrial function and content in the treatment of PA. Membrane potential ($n = 8$ in each group) (A) and total ATP content ($n = 3$ or 4 in each group) (B) of C2C12 cells treated with 200 μM PA in the presence or absence of DHA for 6 or 12 h. Data are normalized to the average of the vehicle-treated group. (C) mtDNA content calculated as the ratio of *COX1* to *Gapdh* DNA levels measured by quantitative PCR in C2C12 cells treated with PA in the presence or absence of DHA ($n = 3$ in each group). (D) Expression of genes for mitochondrial biogenesis and mtDNA replication and repair by quantitative RT-PCR ($n = 4$) after 6 h of treatment. mRNA amounts are expressed relative to the average level of the vehicle-treated group. *, $P < 0.05$; **, $P < 0.01$; ***, $P < 0.001$ (versus vehicle). #$P < 0.05$; ##, $P < 0.01$; ###, $P < 0.001$ (versus PA alone).

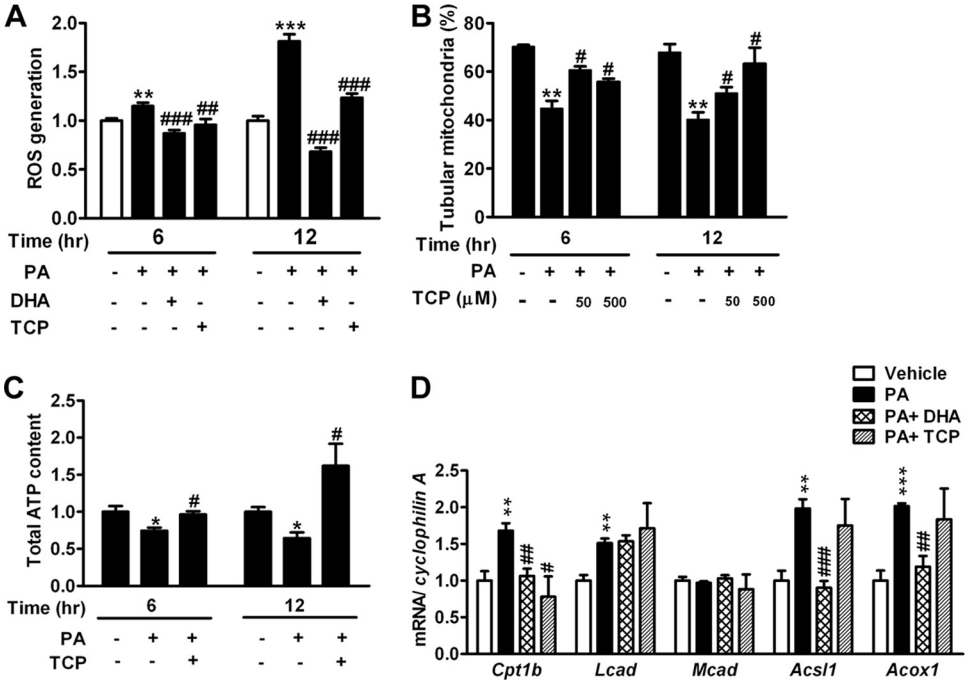

FIG 4 Involvement of ROS in PA-induced mitochondrial fragmentation. (A) Intracellular ROS levels were measured by oxidation of H_2DCFDA in C2C12 cells treated with 200 μM PA, as well as in the group cotreated with DHA (200 μM) or TCP (500 μM), for 6 or 12 h. $n = 8$ in each group. Percentages of tubular mitochondria (B) and total ATP contents (C) in C2C12 cells treated with PA in the presence or absence of TCP for 6 or 12 h are shown. (D) Expression of genes related to FA oxidation by quantitative RT-PCR ($n = 4$) after 6 h of treatment. mRNA amounts are expressed relative to the average level of the vehicle-treated group. *, $P < 0.05$; **, $P < 0.01$; ***, $P < 0.001$ (versus vehicle). #, $P < 0.05$; ##, $P < 0.01$; ###, $P < 0.001$ (versus PA alone).

replication and repair, including single-stranded DNA binding protein 1 (*Ssbp1*) and polymerase gamma 2 (*Polg2*), was increased by PA treatment and reversed by cotreatment with DHA (Fig. 3D). These results suggest that PA-induced mitochondrial fragmentation and dysfunction are not the consequence of reduced mitochondrial content and biogenesis. On the contrary, the decrease in mitochondrial function upon PA exposure was compensated by upregulation of genes related to mitochondrial biogenesis and mtDNA replication and repair.

Involvement of ROS in PA-induced mitochondrial fragmentation. Because ROS has been suggested as a mediator in mitochondrial fragmentation in other cell types (26, 48), we next investigated whether ROS is involved in PA-induced mitochondrial fragmentation in C2C12 cells. First, we observed that treatment with PA significantly increased intracellular ROS levels, reflected by staining with the fluorescent probe H_2DCFDA. Cotreatment with DHA or α-tocopherol (TCP), a ROS scavenger, significantly attenuated the increased ROS levels induced by PA (Fig. 4A). Interestingly, cotreatment with TCP ameliorated PA-induced mitochondrial fragmentation (Fig. 4B). The amelioration of PA-induced mitochondrial fragmentation by cotreatment with TCP was associated with the recovery of ATP production efficiency (Fig. 4C). Thus, our data indicated that attenuation of ROS generation protected against PA-induced mitochondrial fragmentation and dysfunction, implicating a link between ROS generation and mitochondrial fragmentation. To examine whether PA-induced ROS generation is the consequence of changes in FA oxidation, we measured the expression of genes related to FA oxidation. Except for medium-chain acyl coenzyme A (acyl-CoA) dehydrogenase (*Mcad*), the expression of carnitine palmitoyltransferase 1b (*Cpt1b*), long-chain acyl-CoA dehydrogenase (*Lcad*), long-chain fatty acid CoA ligase 1 (*Acsl1*), and acyl-CoA oxidase 1 (*Acox1*) was significantly increased by PA treatment. While cotreatment with DHA significantly ameliorated the PA-induced expression of *Cpt1b*, *Acsl1*, and *Acox1*, cotreatment with TCP only attenuated the PA-induced expression of *Cpt1b* (Fig. 4D).

Increased mitochondrion-associated Drp1 and Fis1 under PA treatment. To determine which components of the mitochondrial fusion and fission machinery mediated mitochondrial fragmentation under PA treatment, we isolated mitochondria from PA-treated C2C12 cells and performed immunoblot analysis. While no difference in the levels of mitochondrion-associated proteins Mfn1, Mfn2, and Opa1 was detected between PA- and vehicle-treated C2C12 cells, the levels of mitochondrion-associated proteins Drp1 and Fis1 were greatly increased in the PA-treated group (Fig. 5A). These results indicated that the component regulating mitochondrial fission was increased by treatment with PA, contributing to the imbalance in mitochondrial dynamics favoring fission.

Attenuation of PA-induced mitochondrial dysfunction and reduction in cellular glucose metabolism by inhibition of mitochondrial fission. We next asked whether inhibition of Drp1 by genetic manipulation would attenuate PA-induced mitochondrial fragmentation and dysfunction. Overexpression of dominant negative Drp1 (DN-Drp1; Drp1-K38A) or Drp1 protein level downregulation by *Drp1* shRNA (Fig. 5B) significantly restored PA-induced mitochondrial fragmentation (Fig. 5C and F) and mitochondrial depolarization (Fig. 5D and G). To directly address whether PA-induced mitochondrial fragmentation is correlated

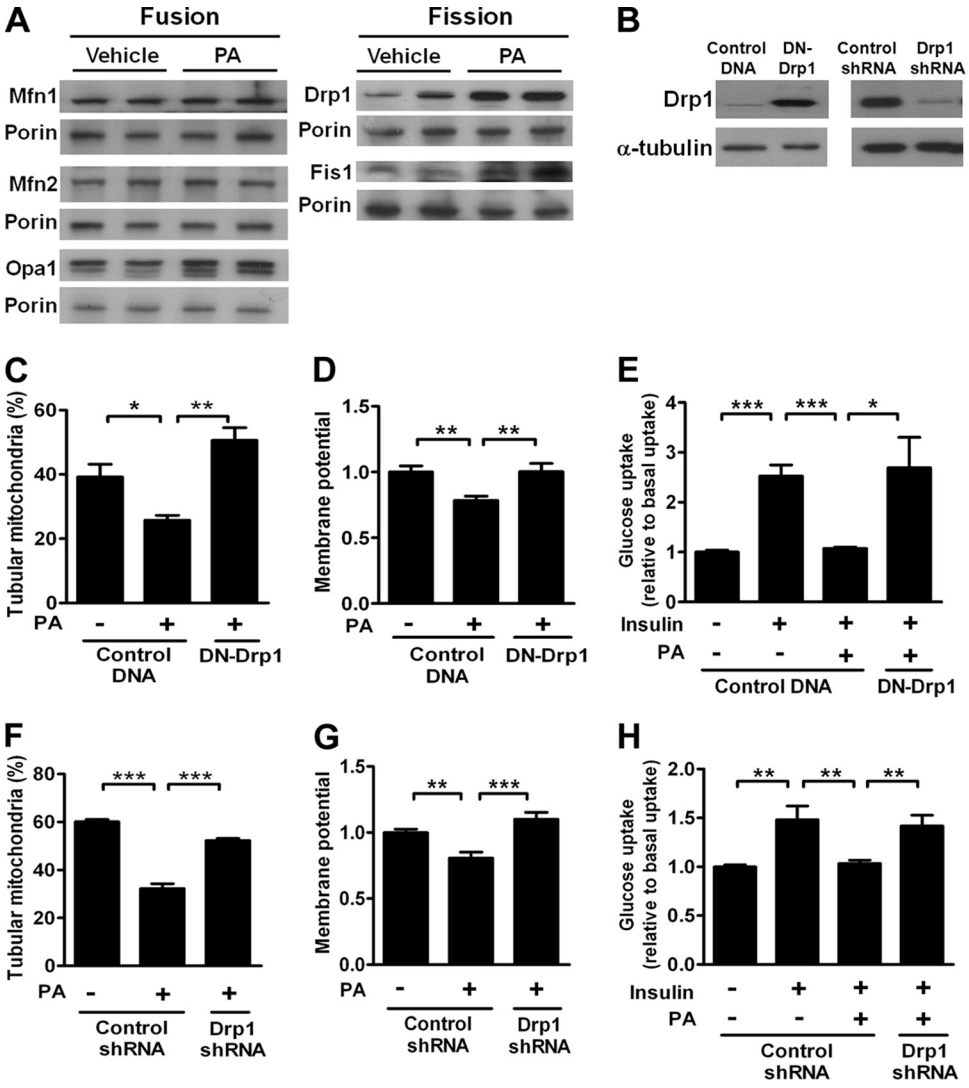

FIG 5 Changes in protein levels and effects of genetically inhibiting Drp1 in PA-treated C2C12 cells. (A) Immunoblot analyses of protein content from the mitochondrial fraction of C2C12 cells treated with 200 μM PA. Porin was used as a loading control for mitochondrial extracts. (B) Protein levels of overexpressed DN-Drp1 (left panel) and effect of Drp1 knockdown (right panel) in C2C12 cells. (C) Percentages of DsRed2-Mito-labeled C2C12 cells displaying tubular mitochondria after transfection with DN-Drp1 plasmids. Results are averages of four individual experiments with at least 100 cells per treatment group in each experiment. (D) Membrane potential of C2C12 cells transfected with DN-Drp1 or control plasmids. $n = 7$ in each group. Data are normalized to the average of the vehicle-treated cells transfected with control plasmids. (E) Quantification of uptake of a fluorescent glucose analog in C2C12 cells transfected with DN-Drp1 or control plasmids. $n = 6$ in each treatment group. Results are normalized to the average of basal uptake. Also shown are percentages of tubular mitochondria (F), membrane potentials (G), and uptake of a florescent glucose analog (H) in C2C12 cells transfected with a *Drp1*-specific shRNA or a control shRNA plasmid. Results in panel F are averages of three individual experiments with at least 100 cells per treatment group in each experiment. $n = 8$ in each treatment group in panels G and H. *, $P < 0.05$; **, $P < 0.01$; ***, $P < 0.001$.

with cellular metabolic deterioration, we examined glucose uptake under insulin stimulation in C2C12 cells. While the presence of PA significantly decreased insulin-stimulated glucose uptake in C2C12 cells, inhibition or knockdown of Drp1 restored the PA-induced reduction of insulin-stimulated glucose uptake (Fig. 5E and H).

Mdivi-1 is a chemical compound which attenuates mitochondrial fission by selectively blocking GTPase activity of Drp1 (7) and provides the potential for therapeutic use. Although treatment with Mdivi-1 partially reversed PA-induced mitochondrial fragmentation (Fig. 6A), it effectively ameliorated PA-induced ROS generation and mitochondrial depolarization, as well as PA-induced reduction of insulin-stimulated glucose uptake, in a dose-dependent manner (Fig. 6B to D). Thus, inhibition of mitochondrial fission attenuates PA-induced mitochondrial fragmentation, ROS generation, mitochondrial depolarization, and suppression of insulin-stimulated glucose uptake.

Altered mitochondrial morphology and proteins involved in mitochondrial dynamics in the skeletal muscle of obese mice. We next studied whether mitochondrial fission was exhibited in skeletal muscle *in vivo* in response to metabolic overload. Three-month-old *ob*/*ob* mice exhibited morbid obesity and severe insulin resistance (data not shown). Similarly, HF treatment of wild-type C57BL/6 mice for 10 weeks resulted in increased body and fat

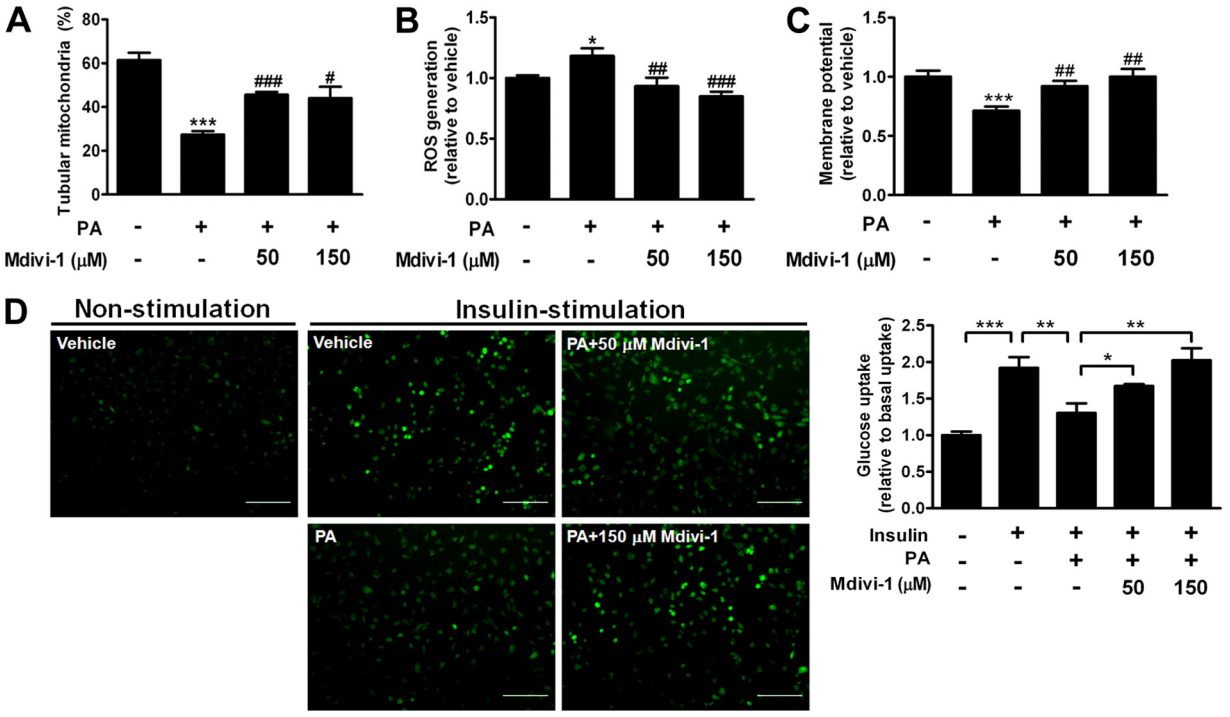

FIG 6 Effects of pharmacological inhibition of mitochondrial fission *in vitro*. Shown are the percentages of tubular mitochondria (A), intracellular ROS levels (B), and membrane potentials (C) of C2C12 cells treated with 200 μM PA in the presence or absence of various concentrations of the mitochondrial fission inhibitor Mdivi-1. $n = 8$ in each treatment group in panels B and C. *, $P < 0.05$; ***, $P < 0.001$ (versus vehicle). #, $P < 0.05$; ##, $P < 0.01$; ###, $P < 0.001$ (versus PA alone). (D) Representative images (left panels) and quantification (right panel) of uptake of a florescent glucose analog in C2C12 cells treated with 200 μM PA in the presence or absence of various concentrations of Mdivi-1 for 6 h. The scale bar is 200 μm. $n = 14$ in each treatment group. Results are normalized to the average basal uptake. *, $P < 0.05$; **, $P < 0.01$; ***, $P < 0.001$.

weight, hyperglycemia, hyperinsulinemia, and increased plasma FFA and triglyceride levels compared to those of LF-fed mice (data not shown). Both mice with genetically induced obesity (*ob*/*ob*) (Fig. 7A and B) and those with HF diet-induced obesity (data not shown) exhibited smaller and shorter mitochondria in the gastrocnemius skeletal muscle than those from the respective control lean mice. To further evaluate whether this phenomenon was associated with proteins involved in mitochondrial dynamics, we measured protein levels in the mitochondrial fraction from the gastrocnemius muscles of obese and lean mice. No difference in the levels of mitochondrion-associated proteins Mfn1, Mfn2, and Opa1 in *ob*/*ob* mice was observed compared to those of the control lean mice (Fig. 7C). Drp1 and Fis1 were significantly increased in the mitochondrial fraction of *ob*/*ob* mouse muscle. Consistently, levels of proteins related to mitochondrial fusion, including Mfn1, Mfn2, and Opa1, were not altered in muscles from HF-fed mice (Fig. 7D). While the Drp1 level was not altered in the mice fed an HF diet for 10 weeks, it was significantly increased in the mice fed an HF diet for 16 weeks (Fig. 7E). The Fis1 level was significantly increased in the mitochondrial fraction of the muscles from mice fed an HF diet for both 10 and 16 weeks.

Improved muscle insulin resistance by inhibition of mitochondrial fission in obese animals. We further tested the effects of inhibiting mitochondrial fission on the skeletal muscle of *ob*/*ob* mice. Treatment of *ob*/*ob* mice with 44 mg/kg Mdivi-1 prior to insulin stimulation increased the insulin-stimulated phosphorylation at Tyr608 of IRS-1, Ser473 of protein kinase B (Akt), and Ser21 of GSK-3α, compared to that in the vehicle-treated group (Fig. 8A). Furthermore, we performed the oral glucose tolerance test (OGTT) to assess the effect of Mdivi-1 on whole-body glucose metabolism. Although the treatment of Mdivi-1 did not change the clearance of glucose after a glucose load, it modestly decreased plasma insulin levels during the OGTT (Fig. 8B). The insulin resistance index calculated from the OGTT was significantly lower in the Mdivi-1-treated *ob*/*ob* mice than in the vehicle-treated *ob*/*ob* mice. Thus, the inhibition of mitochondrial fission machinery by a pharmacological inhibitor improved insulin signaling in the skeletal muscle and systemic insulin sensitivity in *ob*/*ob* mice.

Attenuation of protein kinases by inhibition of mitochondrial fission in obese animals. To address how changes in mitochondrial morphology can modulate the insulin signaling pathway, we detected several serine/threonine protein kinases that are known to be activated by intracellular lipid metabolites and ROS and inhibit insulin signaling. The phosphorylation of ERK1/2 and p38 mitogen-activated protein kinase (MAPK) was increased in the skeletal muscle of *ob*/*ob* mice, compared to that of control mice (Fig. 9A). Mdivi-1 treatment attenuated the increased phosphorylation of ERK1/2 and p38 in the skeletal muscle of *ob*/*ob* mice. No difference in the phosphorylation of JNK was detectable among the three groups. We further examine the role of FA oxidation in the skeletal muscle of *ob*/*ob* mice. The expression of *Cpt1b*, *Lcad*, *Mcad*, and *Acsl1* was upregulated in the skeletal muscle of *ob*/*ob* mice, whereas Mdivi-1 treatment showed a tendency to restore the increased gene expression in *ob*/*ob* mice (Fig. 9B).

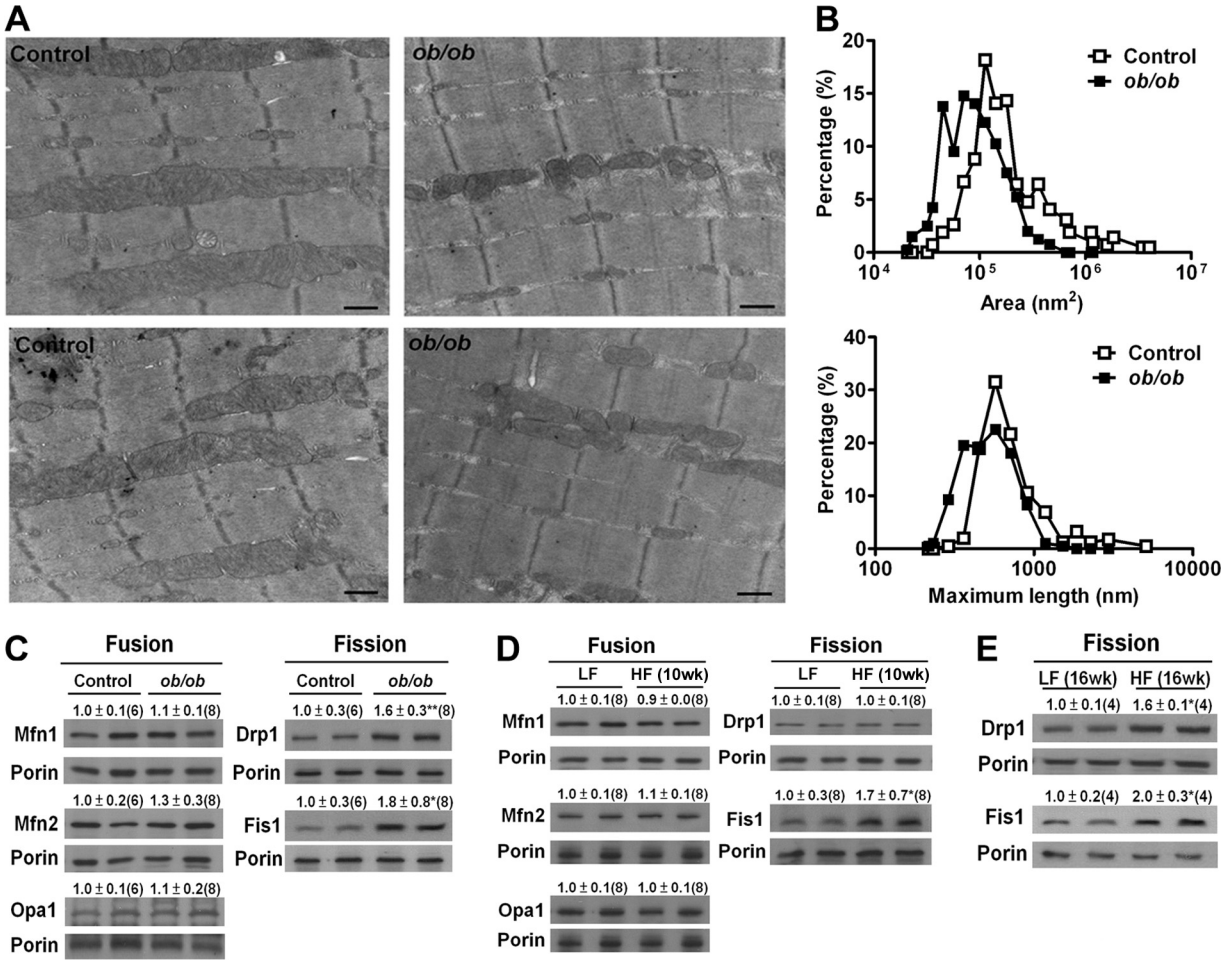

FIG 7 Mitochondrial morphology and proteins related to mitochondrial dynamics in the skeletal muscles of obese mice. (A) Mitochondrial morphology imaged by transmission electron microscopy. (B) Distribution of mitochondrial areas and lengths in the gastrocnemius muscles of *ob*/*ob* and control mice. Each scale bar is 500 nm. Also shown are immunoblot analyses of the protein contents of the mitochondrial fraction of the muscle tissues of *ob*/*ob* and control mice at the age of 13 weeks (C), mice fed HF and LF diets for 10 weeks (D), and mice fed HF and LF diets for 16 weeks (E). Samples from representative animals are shown in the Western blot assay, with each lane representing one animal. The intensities of the bands, quantified densitometrically relative to that of the respective controls, are shown with the sample number in parentheses. *, $P < 0.05$; **, $P < 0.01$. Porin was used as a loading control for mitochondrial extracts.

DISCUSSION

The idea that disruption of mitochondrial dynamics underlies the pathogenesis of metabolism-related diseases is gaining support. For example, two studies demonstrated that an imbalance of mitochondrial networks in neurons favoring mitochondrial fission plays a critical role in the pathogenesis of diabetic neuropathy both *in vivo* and *in vitro* (14, 45). Another study revealed mitochondrial fragmentation in coronary endothelial cells from di-

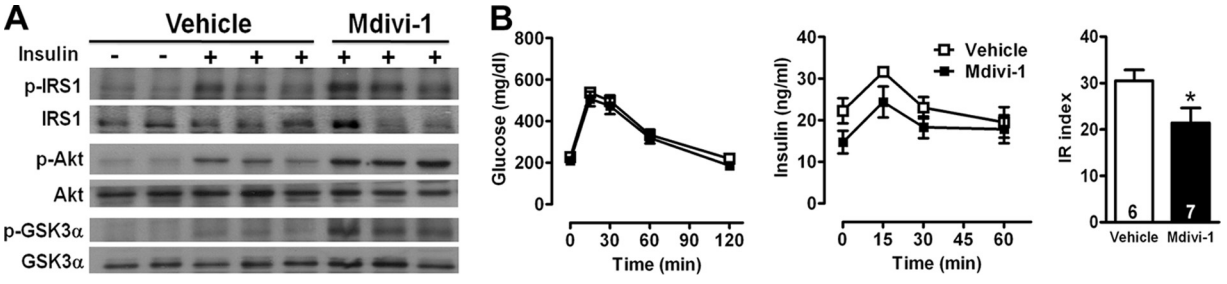

FIG 8 Effects of mitochondrial fission inhibition *in vivo*. (A) Immunoblot analyses of phosphorylation at Tyr608 of IRS-1, Ser473 of Akt, and Ser21 of GSK-3α from the whole lysate of gastrocnemius muscles of *ob*/*ob* mice under Mdivi-1 treatment. Muscle tissues were collected 2 min after injection with 5 U/kg insulin through the vena cava for analyses of phosphorylation. Each band represents a tissue extract from a single mouse. (B) Plasma glucose (left panel) and insulin (middle panel) levels and insulin resistance (IR) indexes (right panel) during OGTT in 13-week-old *ob*/*ob* mice that received Mdivi-1 ($n = 7$) or vehicle ($n = 6$). *, $P < 0.05$ (versus vehicle).

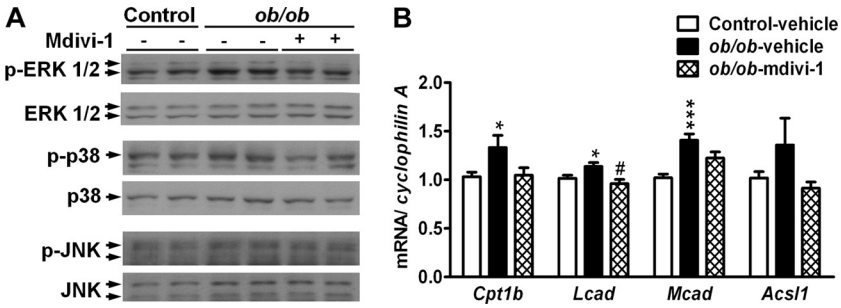

FIG 9 Protein kinases and FA oxidation in the skeletal muscles of obese mice. (A) Immunoblot analysis of ERK1/2, p38, and JNK phosphorylation in the skeletal muscles of control and *ob*/*ob* mice treated with vehicle or Mdivi-1. (B) Expression of genes related to FA oxidation by quantitative RT-PCR. A group of control mice ($n = 9$) received the vehicle (Control-vehicle), a group of *ob*/*ob* mice ($n = 5$) received the vehicle (*ob*/*ob*-vehicle), and a group of *ob*/*ob* mice ($n = 7$) received Mdivi-1 (*ob*/*ob*-Mdivi-1). mRNA amounts are expressed relative to the average level of the vehicle-received control mice. *, $P < 0.05$; ***, $P < 0.001$ (versus control vehicle). #, $P < 0.05$ (versus *ob*/*ob*-vehicle).

abetic mice (26). Several types of cultured cells from the cardiovascular system exhibited mitochondrial fission under hyperglycemic conditions (48). These studies all support the notion that sustained hyperglycemia is the cause of mitochondrial fission. Alteration of mitochondrial morphology was also reported to mediate tissue injury upon ischemic stress. For example, mitochondrial fission occurs in the kidneys and heart after acute ischemia/reperfusion injury in mice, and prevention of this process is beneficial (5, 32). Finally, exposure to high levels of glucose and PA induced pancreatic β-cell mitochondrial fragmentation, and preserving mitochondrial dynamics protected β cells from apoptosis (28, 29). Thus, the fine balance between mitochondrial fusion and fission can be upset by a variety of stress responses, including nutrient stress and simulated ischemia. Furthermore, amelioration of imbalanced mitochondrial dynamics reduces cellular damage and disease severity, highlighting the importance of mitochondrial dynamics in the pathogenesis of diseases of the neurons, heart, kidneys, and β cells, which rely heavily on functional, healthy mitochondria.

Our results suggest that the fusion machinery is not much affected in the skeletal muscle of obese rodents or in PA-treated C2C12 cells. Instead, the fission machinery is likely the main component involved in the regulation of mitochondrial dynamics in our *in vivo* and *in vitro* models. In agreement with our hypothesis, fusion-related proteins, including Mfn1, Mfn2, and Opa1, were not changed in the muscles of mice with *ob*/*ob*- or HF-induced obesity or in PA-treated C2C12 cells. In contrast, the fission-related protein Fis1 was significantly increased both in muscles from obese rodents and in PA-treated C2C12 cells. Another fission-related protein, Drp1, was increased in PA-treated C2C12 cells and in muscles from *ob*/*ob* mice and mice fed an HF diet for 16 weeks but not altered in muscles from mice fed an HF diet for 10 weeks. The lack of a detectable increase in mitochondrion-associated Drp1 in muscles from mice fed an HF diet for 10 weeks may be due to the relatively lower body weight increase in mice fed an HF diet for 10 weeks (mean body weight of 39 g in mice fed an HF diet for 10 weeks versus 28 g in those fed an LF diet) than in *ob*/*ob* mice (56 g in *ob*/*ob* mice versus 26 g in control mice) and mice fed an HF diet for 16 weeks (48 g in mice fed an HF diet for 16 weeks versus 29 g in those fed an LF diet). Thus, it is possible that the increase in the mitochondrion-associated Drp1 level is correlated with the degree of body weight increase. Nevertheless, the consistent increases of mitochondrion-associated Fis1 both *in vivo* and *in vitro* support the idea that mitochondria are equipped with fission machinery under this circumstance. These findings further suggest that Fis1, at least in part, is the cause of increased mitochondrial fission in the muscle of obese mice and PA-treated cultured muscle cells.

Mdivi-1 attenuates mitochondrial fragmentation by selectively inhibiting the assembly and GTPase activity of Drp1 (7). It affects neither the GTPase activity of dynamin 1 nor that of yeast homologs of Mfn1/2 and Opa1. In our study, inhibition of Drp1 by Mdivi-1 *in vitro* rescued PA-mediated mitochondrial injuries, as indicated by diminished mitochondrial depolarization and ROS generation. Consistently, we found that inhibition of Drp1 rendered C2C12 cells resistant to PA-mediated suppression of insulin-stimulated glucose transport. Furthermore, Drp1 inhibition with Mdivi-1 ameliorated the impairment of insulin signal transduction in obese rodent muscle. The fact that mitochondrion-associated Drp1 was increased in *ob*/*ob* mouse muscle might explain the efficacy of the direct inhibition of Drp1 GTPase activity with Mdivi-1 in the attenuation of metabolic deterioration *in vivo*.

In the search for extracellular stimuli that induce mitochondrial fission, we did not detect an effect of hyperglycemia, hyperinsulinemia, or elevated TNF-α at supraphysiological and pathological concentrations on changes in mitochondrial morphology. In humans, the average concentration of FFAs in the postabsorptive state is 500 to 1,000 μM in the plasma, and that of PA can reach 200 μM (17). Although many studies demonstrated the effect of hyperglycemia on increased generation of ROS and mitochondrial fission in a variety of cell types (26, 48), elevated circulating lipid and inflammatory cytokines usually occur prior to the development of hyperinsulinemia and hyperglycemia during the progression of type 2 diabetes (27, 38). Lipid overload impairs oxidative capacity and increases the intracellular accumulation of FA-derived metabolites, such as long-chain acyl-CoA, diacylglycerol, ceramide, and triacylglycerol, in skeletal muscle (1, 30, 35, 37). These metabolites are associated with insulin resistance by impairing the insulin-signaling pathways. Thus, our results provide a rationale for the development of muscle insulin resistance in response to lipid flux.

In the time course study, we found similar effects of PA on the alteration of mitochondrial morphology when cells were treated with 200 μM PA for 24 or 48 h (data not shown). Because cell toxicity, examined by lactate dehydrogenase assay and crystal vi-

olet stain, was exhibited at 48 h of treatment with 200 μM PA (data not shown), we performed treatment for 6 or 12 h in this study. Similarly, no evidence of apoptosis, revealed by immunoblotting of cleaved caspase 3, was observed in cells treated with 200 μM PA for 6 h (data not shown). Thus, our data suggest that PA does not largely affect signaling and cellular processes that could be linked to cellular death under the experimental conditions and time course we studied.

In our study, we noticed that the results from muscle cells are in acute treatments whereas data from animals are due to chronic effects. A speculation on the association between acute HF feeding and mitochondrial morphology *in vivo* is raised. Short-term lipid infusion for 6 to 8 h in healthy individuals does not change mitochondrial content, morphology, and respiration rates in skeletal muscle despite a lower mitochondrial membrane potential (4, 10). Similarly, HF feeding of mice for 4 weeks does not alter their mitochondrial content and respiration rates (3). These findings suggest that acute HF feeding might not have the same effect on mitochondrial morphology and dysfunction prior to demonstrable obesity. However, this still leaves the question of whether the findings obtained in culture are relevant to adult muscle tissue in this study. For example, the muscle tissue, with the myocytes and other accessory cells, in obese mice encountered long-term excess FFAs, as well as other nutrient and inflammatory stimuli. The effect *in vivo* is also influenced by inputs from other organs. In contrast, the cultured cells encountered relatively short-term excess FFAs alone. Nevertheless, our results at least suggest that the exposure of muscle cells to PA is deleterious to mitochondrial architecture.

It is generally recognized that saturated, unsaturated, and polyunsaturated FAs mediate quite diverse effects. For example, saturated FAs reduce mitochondrial membrane potential, as well as ATP generation, in C2C12 cells, while unsaturated and ω-3 polyunsaturated FFAs do not alter these functions (21). Comparisons of several FAs yielded interesting findings in our study. For example, while the saturated FAs MA and PA induced mitochondrial fission, SA had no effect despite being only two carbon atoms longer than PA. None of the unsaturated or polyunsaturated FAs we tested affected mitochondrial fission. Interestingly, cotreatment with unsaturated and polyunsaturated FAs alleviated PA-induced mitochondrial fission. Thus, the diverse effects of different FAs on mitochondrial morphology correlated with their impacts on mitochondrial and cellular functions. Furthermore, unsaturated FAs added to the diet have protective effects against metabolic disorders. For example, supplementation of eicosapentaenoate and DHA protects mice from HF-induced body weight gain, dyslipidemia, and glucose intolerance (23). Dietary supplementation with monounsaturated FAs improves insulin sensitivity and adipokine and lipid profiles in the HF-fed mice and healthy young subjects (44, 47). Although no evidence directly addresses the relationship between dietary unsaturated FAs and *in vivo* mitochondrial morphology, our results, together with those of other studies, suggest that supplementation with unsaturated FAs can reverse insulin resistance and *in vivo* mitochondrial morphology defects.

The relationship between FA oxidation and mitochondrial function remains unclear. While reduced FA oxidation was observed in obese human muscle (39, 42), increased FA oxidation in muscle tissue was found in several HF-fed rodent models (19, 43). Our data showed that genes related to FA oxidation were upregulated in PA-treated cells and *ob*/*ob* mouse muscles, suggesting that FA oxidation is increased in response to PA or lipid overload. Thus, it is likely that excessive FA oxidation due to lipid overload leads to the formation of free radicals and ROS that can compromise mitochondrial function. Interestingly, cotreatment of PA-treated cells with DHA or inhibition of fission by Mdivi-1 in *ob*/*ob* mice reversed upregulated genes, suggesting the attenuation of increased FA oxidation in the presence of DHA or Mdivi-1.

Substantial evidence shows that ROS is a key mechanism linking metabolic disturbance to nutrient excess. Thus, obesity induced by an HF diet leads to enhanced oxidative stress in rodents (3, 46). Our study demonstrated that increased ROS levels in response to excess PA are the direct cause of mitochondrial fragmentation, because decreasing ROS levels with a scavenger prevented PA-induced mitochondrial fission (Fig. 4B). Furthermore, blocking of mitochondrial fission significantly alleviated PA-induced ROS generation (Fig. 6B). These data imply a tight association and interplay between ROS generation and mitochondrial fission. ROS can function as signaling molecules to activate the MAPK family, including ERK, p38, and JNK (15, 25). Other studies demonstrated that activation of these protein kinases phosphorylates IRS-1 at its serine residue(s), which further interrupts tyrosine phosphorylation on IRS-1 and suppresses downstream insulin signaling (12). Thus, our study indicated that ROS resulted from nutrient excess or PA exposure is deleterious to mitochondrial architecture and dynamics in muscle tissue/cells. Imbalance in the mitochondrial dynamics would accelerate ROS accumulation, which may further activate signaling molecules, including the MAPK family, and suppress insulin signaling. Our data showed that obesity increased the phosphorylation of ERK1/2 and p38 in skeletal muscle and that inhibition of mitochondrial fission reversed that and ameliorated insulin resistance. These results support the link between mitochondrial morphology, ROS generation, and activation of the MAPK family in the regulation of the insulin signaling pathway.

In conclusion, we provide evidence that mitochondrial fission occurs in the skeletal muscle of obese animals and in cultured muscle cells in response to high levels of some saturated FAs. Inhibition of mitochondrial fission protected muscle cells against mitochondrial dysfunction and insulin resistance *in vitro* and, more importantly, improved muscle insulin signaling and systemic insulin sensitivity *in vivo*. Thus, our results establish a causative link between mitochondrial dynamics and metabolic deterioration and imply that disruption of mitochondrial dynamics in skeletal muscle may underlie the pathogenesis of insulin resistance. Finally, manipulation of mitochondrial morphology may provide a novel therapeutic strategy for insulin resistance and type 2 diabetes.

ACKNOWLEDGMENTS

We thank I. C. Bruce, A. Pendse, J.-Y. Chen, Y.-H. Wei, and H.-I. Yeh for discussions and S.-H. Huang and H.-T. Wu, Department of Pathology of National Cheng Kung University Hospital and National RNAi Core Facility at Academia Sinica, respectively, for technical assistance.

This work was supported by grants from the National Science Council (NSC-98-2320-B-006-009-MY3) and the National Health Research Institutes (NHRI-EX100-9823SC).

REFERENCES

1. **Abdul-Ghani MA, et al.** 2008. Deleterious action of FA metabolites on ATP synthesis: possible link between lipotoxicity, mitochondrial dysfunc-

tion, and insulin resistance. Am. J. Physiol. Endocrinol. Metab. **295**: E678–E685.
2. **Bonen A, et al.** 2004. Triacylglycerol accumulation in human obesity and type 2 diabetes is associated with increased rates of skeletal muscle fatty acid transport and increased sarcolemmal FAT/CD36. FASEB J. **18**: 1144–1146.
3. **Bonnard C, et al.** 2008. Mitochondrial dysfunction results from oxidative stress in the skeletal muscle of diet-induced insulin-resistant mice. J. Clin. Invest. **118**:789–800.
4. **Brands M, et al.** 2011. Short-term increase of plasma free fatty acids does not interfere with intrinsic mitochondrial function in healthy young men. Metabolism **60**:1398–1405.
5. **Brooks C, Wei Q, Cho SG, Dong Z.** 2009. Regulation of mitochondrial dynamics in acute kidney injury in cell culture and rodent models. J. Clin. Invest. **119**:1275–1285.
6. **Cartoni R, et al.** 2005. Mitofusins 1/2 and ERRalpha expression are increased in human skeletal muscle after physical exercise. J. Physiol. **567**: 349–358.
7. **Cassidy-Stone A, et al.** 2008. Chemical inhibition of the mitochondrial division dynamin reveals its role in Bax/Bak-dependent mitochondrial outer membrane permeabilization. Dev. Cell **14**:193–204.
8. **Chan DC.** 2006. Mitochondrial fusion and fission in mammals. Annu. Rev. Cell Dev. Biol. **22**:79–99.
9. **Chang CR, Blackstone C.** 2007. Cyclic AMP-dependent protein kinase phosphorylation of Drp1 regulates its GTPase activity and mitochondrial morphology. J. Biol. Chem. **282**:21583–21587.
10. **Chavez AO, et al.** 2010. Effect of short-term free fatty acids elevation on mitochondrial function in skeletal muscle of healthy individuals. J. Clin. Endocrinol. Metab. **95**:422–429.
11. **Chen H, Chomyn A, Chan DC.** 2005. Disruption of fusion results in mitochondrial heterogeneity and dysfunction. J. Biol. Chem. **280**: 26185–26192.
12. **De Fea K, Roth RA.** 1997. Modulation of insulin receptor substrate-1 tyrosine phosphorylation and function by mitogen-activated protein kinase. J. Biol. Chem. **272**:31400–31406.
13. **Detmer SA, Chan DC.** 2007. Functions and dysfunctions of mitochondrial dynamics. Nat. Rev. Mol. Cell Biol. **8**:870–879.
14. **Edwards JL, et al.** 2010. Diabetes regulates mitochondrial biogenesis and fission in mouse neurons. Diabetologia **53**:160–169.
15. **Evans JL, Goldfine ID, Maddux BA, Grodsky GM.** 2003. Are oxidative stress-activated signaling pathways mediators of insulin resistance and beta-cell dysfunction? Diabetes **52**:1–8.
16. **Frank S, et al.** 2001. The role of dynamin-related protein 1, a mediator of mitochondrial fission, in apoptosis. Dev. Cell **1**:515–525.
17. **Fraser DA, Thoen J, Rustan AC, Forre O, Kjeldsen-Kragh J.** 1999. Changes in plasma free fatty acid concentrations in rheumatoid arthritis patients during fasting and their effects upon T-lymphocyte proliferation. Rheumatology (Oxford) **38**:948–952.
18. **Guilherme A, Virbasius JV, Puri V, Czech MP.** 2008. Adipocyte dysfunctions linking obesity to insulin resistance and type 2 diabetes. Nat. Rev. Mol. Cell Biol. **9**:367–377.
19. **Hancock CR, et al.** 2008. High-fat diets cause insulin resistance despite an increase in muscle mitochondria. Proc. Natl. Acad. Sci. U. S. A. **105**: 7815–7820.
20. **Hegarty BD, Cooney GJ, Kraegen EW, Furler SM.** 2002. Increased efficiency of fatty acid uptake contributes to lipid accumulation in skeletal muscle of high fat-fed insulin-resistant rats. Diabetes **51**:1477–1484.
21. **Hirabara SM, Curi R, Maechler P.** 2010. Saturated fatty acid-induced insulin resistance is associated with mitochondrial dysfunction in skeletal muscle cells. J. Cell. Physiol. **222**:187–194.
22. **Kelley DE, He J, Menshikova EV, Ritov VB.** 2002. Dysfunction of mitochondria in human skeletal muscle in type 2 diabetes. Diabetes **51**: 2944–2950.
23. **Kuda O, et al.** 2009. n-3 fatty acids and rosiglitazone improve insulin sensitivity through additive stimulatory effects on muscle glycogen synthesis in mice fed a high-fat diet. Diabetologia **52**:941–951.
24. **Lowell BB, Shulman GI.** 2005. Mitochondrial dysfunction and type 2 diabetes. Science **307**:384–387.
25. **Maddux BA, et al.** 2001. Protection against oxidative stress-induced insulin resistance in rat L6 muscle cells by micromolar concentrations of alpha-lipoic acid. Diabetes **50**:404–410.
26. **Makino A, Scott BT, Dillmann WH.** 2010. Mitochondrial fragmentation and superoxide anion production in coronary endothelial cells from a mouse model of type 1 diabetes. Diabetologia **53**:1783–1794.
27. **McGarry JD.** 2002. Banting lecture 2001: dysregulation of fatty acid metabolism in the etiology of type 2 diabetes. Diabetes **51**:7–18.
28. **Men X, et al.** 2009. Dynamin-related protein 1 mediates high glucose induced pancreatic beta cell apoptosis. Int. J. Biochem. Cell Biol. **41**: 879–890.
29. **Molina AJ, et al.** 2009. Mitochondrial networking protects beta-cells from nutrient-induced apoptosis. Diabetes **58**:2303–2315.
30. **Montell E, et al.** 2001. DAG accumulation from saturated fatty acids desensitizes insulin stimulation of glucose uptake in muscle cells. Am. J. Physiol. Endocrinol. Metab. **280**:E229–E237.
31. **Muoio DM, Newgard CB.** 2008. Mechanisms of disease: molecular and metabolic mechanisms of insulin resistance and beta-cell failure in type 2 diabetes. Nat. Rev. Mol. Cell Biol. **9**:193–205.
32. **Ong SB, et al.** 2010. Inhibiting mitochondrial fission protects the heart against ischemia/reperfusion injury. Circulation **121**:2012–2022.
33. **Parone PA, et al.** 2008. Preventing mitochondrial fission impairs mitochondrial function and leads to loss of mitochondrial DNA. PLoS One **3**:e3257.
34. **Petersen KF, Dufour S, Befroy D, Garcia R, Shulman GI.** 2004. Impaired mitochondrial activity in the insulin-resistant offspring of patients with type 2 diabetes. N. Engl. J. Med. **350**:664–671.
35. **Powell DJ, Turban S, Gray A, Hajduch E, Hundal HS.** 2004. Intracellular ceramide synthesis and protein kinase Czeta activation play an essential role in palmitate-induced insulin resistance in rat L6 skeletal muscle cells. Biochem. J. **382**:619–629.
36. **Ritov VB, et al.** 2005. Deficiency of subsarcolemmal mitochondria in obesity and type 2 diabetes. Diabetes **54**:8–14.
37. **Sabin MA, et al.** 2007. Fatty acid-induced defects in insulin signalling, in myotubes derived from children, are related to ceramide production from palmitate rather than the accumulation of intramyocellular lipid. J. Cell. Physiol. **211**:244–252.
38. **Schenk S, Saberi M, Olefsky JM.** 2008. Insulin sensitivity: modulation by nutrients and inflammation. J. Clin. Invest. **118**:2992–3002.
39. **Simoneau JA, Veerkamp JH, Turcotte LP, Kelley DE.** 1999. Markers of capacity to utilize fatty acids in human skeletal muscle: relation to insulin resistance and obesity and effects of weight loss. FASEB J. **13**:2051–2060.
40. **Sparks LM, et al.** 2005. A high-fat diet coordinately downregulates genes required for mitochondrial oxidative phosphorylation in skeletal muscle. Diabetes **54**:1926–1933.
41. **Suen DF, Norris KL, Youle RJ.** 2008. Mitochondrial dynamics and apoptosis. Genes Dev. **22**:1577–1590.
42. **Thyfault JP, et al.** 2004. Impaired plasma fatty acid oxidation in extremely obese women. Am. J. Physiol. Endocrinol. Metab. **287**:E1076–E1081.
43. **Turner N, et al.** 2007. Excess lipid availability increases mitochondrial fatty acid oxidative capacity in muscle: evidence against a role for reduced fatty acid oxidation in lipid-induced insulin resistance in rodents. Diabetes **56**:2085–2092.
44. **Uusitupa M, et al.** 1994. Effects of two high-fat diets with different fatty acid compositions on glucose and lipid metabolism in healthy young women. Am. J. Clin. Nutr. **59**:1310–1316.
45. **Vincent AM, et al.** 2010. Mitochondrial biogenesis and fission in axons in cell culture and animal models of diabetic neuropathy. Acta Neuropathol. **120**:477–489.
46. **Wellen KE, Thompson CB.** 2010. Cellular metabolic stress: considering how cells respond to nutrient excess. Mol. Cell **40**:323–332.
47. **Yang ZH, Miyahara H, Mori T, Doisaki N, Hatanaka A.** 2011. Beneficial effects of dietary fish-oil-derived monounsaturated fatty acids on metabolic syndrome risk factors and insulin resistance in mice. J. Agric. Food Chem. **59**:7482–7489.
48. **Yu T, Sheu SS, Robotham JL, Yoon Y.** 2008. Mitochondrial fission mediates high glucose-induced cell death through elevated production of reactive oxygen species. Cardiovasc. Res. **79**:341–351.